Clinical Radiology 74 (2019) 406.e19–406.e27

Contents lists available at ScienceDirect

Clinical Radiology

journal homepage: www.clinicalradiologyonline.net

Questionable correlation of the apparent diffusion coefficient with the histological grade and microvascular invasion in small hepatocellular carcinoma

J.G. Kim [a], K.M. Jang [a,*], G.S. Min [b], T.W. Kang [a], D.I. Cha [a], S.H. Ahn [c]

[a] *Department of Radiology, Samsung Medical Center, Sungkyunkwan University School of Medicine, Seoul, Republic of Korea*

[b] *Eone Pathology Laboratory, Seongnam-si, Gyeonggi-do, Republic of Korea*

[c] *Mathematics, Ajou University, Yeongtong-gu, Suwon-si, Gyeonggi-do, Republic of Korea*

ARTICLE INFORMATION

Article history:
Received 26 June 2018
Accepted 24 January 2019

AIM: To evaluate the correlation between the apparent diffusion coefficient (ADC) and various histopathological parameters in small hepatocellular carcinomas (HCCs).

MATERIALS AND METHODS: In 143 surgically resected small HCCs, the mean and minimum ADC values, tumour-to-liver ADC ratio, and normalised ADC (ADC of the HCC/ADC of the spleen) were correlated to the tumour grade, microvascular invasion (MVI), cellularity, fatty change, degree of fibrosis, and lymphocytic infiltration using linear regression analysis, the Wilcoxon rank sum test, or Spearman's rank correlation.

RESULTS: No significant correlation was found between the ADC parameters and tumour grade. In the univariate analysis, the ADC ratio of the tumour was significantly correlated with MVI as well as the degree of fibrosis and lymphocyte infiltration of the HCC (p=0.017, 0.042, and 0.002, respectively). The ADC of the tumour was significantly correlated with the degree of lymphocyte infiltration of the HCC (p=0.049). In the multivariate analysis, the ADC ratio of the tumour was an independent parameter for MVI and the degree of lymphocyte infiltration of the HCC (p=0.034 and <0.001, respectively), and the ADC of the tumour was an independent parameter for the degree of lymphocyte infiltration of the HCC (p=0.009). There was no significant correlation between the other ADCs and pathological tumour parameters.

CONCLUSION: The tumour grade of small HCCs was not correlated with ADC parameters. The tumour-to-liver ADC ratio was a significant independent parameter for the degree of lymphocyte infiltration and MVI of small HCCs.

Introduction

Diffusion-weighted imaging (DWI) is widely used for the detection and evaluation of liver lesions, particularly metastases.[1] DWI is also beneficial in the detection of

* Guarantor and correspondent: K. M. Jang, Department of Radiology, Samsung Medical Center, Sungkyunkwan University School of Medicine, 81 Ilwon-Ro, Gangnam-gu, Seoul, Republic of Korea. Tel.: +82-2-3410-6438; fax: +82-2-3410-2559.

E-mail address: kmmks.jang@samsung.com (K.M. Jang).

https://doi.org/10.1016/j.crad.2019.01.019

hepatocellular carcinomas (HCCs) and differentiation of such from benign focal hepatic lesions.[2,3] An HCC is typically defined as a hyperintense lesion on high b-value (≥500 s/mm^2) DWI with low or iso signal intensity compared to the surrounding liver parenchyma on an apparent diffusion coefficient (ADC) map.[2,4–6]

High-grade tumours generally consist of densely packed cells with a high nuclear-to-cytoplasmic ratio, which is known to inhibit the effective motion of water molecules and lead to restricted diffusion.[7] Among the previous studies on the aggressiveness of HCCs (summarised in Electronic Supplementary Material Appendix E1), some have reported the utility of ADC values for predicting tumour differentiation and the presence of microvascular invasion (MVI),[8–13] whereas others have reported no significant association between the ADC and the histopathological grade or early HCC recurrence.[14–16] One previous study demonstrated that there is a large overlap of ADC values among different histological grades.[14] In addition to tumour cells, HCCs could present with various degrees of fat, fibrosis, lymphocyte infiltration, haemorrhage, or necrosis, which could affect the ADC value of the tumour[17,18]; however, to the authors' knowledge, the association between the aforementioned histopathological components of HCCs and ADC values has not been evaluated. Accordingly, the aim of the present study was to evaluate the association between ADC values and various histopathological features of HCCs.

Material and methods

Study population

The institutional review board approved this retrospective study and the requirement to obtain informed consent from the patient was waived. Via a computerised search of the institutional surgical pathological database between January 2013 and December 2015, patients who met the following inclusion criteria were included in the study: (a) patients with HCCs that were untreated before surgery, (b) patients who underwent liver magnetic resonance imaging (MRI) with DWI according to the standard protocol within 2 months prior to surgery, (c) tumours of ≤20 mm in diameter on pathological analysis, such that the entire tumour can be included in one 2.5 cm-wide pathological cross-section slide, (d) tumours of ≥10 mm in diameter on pathological analysis in order to avoid partial volume effects on imaging, and (e) HCCs that exhibited no slice misregistration among each DWI series. A review of pathological reports and MRI images to determine the eligibility for enrolment in this study was performed by one abdominal radiologist (K.M.J. with 16 years of experience in abdominal MRI interpretation). All MRI images were evaluated on a picture archiving and communication system (PACS, Pathspeed; GE Medical Systems Integrated Imaging Solutions, Mt Prospect, IL, USA), and adjustment of the optimal window setting in each case was conducted by the radiologists who participated in this study.

MRI technique

All MRI images were obtained using a 3 T whole-body MR system (Intera Achieva; Philips Healthcare, Best, the Netherlands) with a 32-channel phased-array (torso and/or cardiac) coil as the receiver coil. DWI images with b-values of 0, 100, and 800 s/mm^2 were acquired before the administration of the contrast agent using respiratory-triggered single-shot echo planar imaging that was applied within the same acquisition along the three orthogonal directions of the motion-probing gradients. The spectral pre-saturation with inversion recovery for fat suppression technique, no half scan, and sensitivity encoding acceleration factor of 4.0 were used. The start of each acquisition was timed to the same state of the respiratory cycle. The ADC was calculated using a mono-exponential function with b-values of 0 and 800 s/mm^2. ADC maps were automatically constructed on a pixel-by-pixel basis using MRI station software. Details regarding the acquisition of baseline MRI sequences and gadoxetic acid (Primovist; Bayer Schering Pharma, Berlin, Germany) enhanced images are provided in Table 1.

ADC analysis

At the first session, the mean ADC value was measured on an ADC map by one radiologist (T.W.K. with 9 years of experience in abdominal MRI interpretation). The ADC value was automatically calculated by the computer software included with the GE workstation. ADC values were measured in the mid-section of the tumour to minimise partial volume averaging effects and motion artefacts. The largest possible circular or ovoid free-hand regions of interest (ROIs), devoid of frank necrosis and haemorrhagic foci, were applied to the tumours, while avoiding the most

Table 1
Magnetic resonance imaging protocol parameters.

Sequence	TR/TE (ms)	Flip angle (°)	Matrix size	Section thickness (mm)	Intersection gap (mm)	No. of signals
Dual GRE T1W	3.5/1.2–2.3	10	256×194	6	6	1
Breath-hold MST2WI[a]	1476.5/70	90	256×260	5	5	1
Respiratory triggered SS T2WI[a]	1131.3/80	90	376×273	5	5	2
Respiratory triggered SSHT2WI[a]	1328.5/160	90	376×273	5	5	2
DWI[a]	1444/55	90	112×108	5	6	2
3D GRE T1WI[a]	3.1/1.5	10	252×251	4.4	2.2	1

3D, three-dimensional; TR, repetition time; TE, echo time; GRE, gradient echo; MST2WI, multi-shot T2-weighted image; SST2WI, single-shot T2-weighted image; SSHT2WI, single-shot heavily T2-weighted image.
[a] Fat saturation images.

peripheral portions to prevent partial volume effects of the adjacent liver parenchyma. When the tumours were invisible on DWI images or ADC maps, the ADC measurements were performed in the expected tumour area under adjacent correlation of the DWI images, ADC map, and conventional MRI images using a spatial cursor key on the PACS that localises corresponding sites on different images using multiplanar localisation. In addition, the minimum ADC values of the tumours were also measured.[19] The mean ROI for tumours was 61.8 mm^2 (range, 13–175 mm). Meanwhile, ROIs were applied to the surrounding hepatic parenchyma in the same segment with a round-shaped ROI of 10–20 mm in diameter devoid of artefacts and blood vessels. For normalisation of the ADC value of the HCCs, the spleen was used as the reference organ and the ADC value of the spleen was determined. ROIs from three consecutive slices were measured in the central section obtained through the level of the splenic hilum in each case using a similar method to that used for liver parenchyma.[20] The ADC values of the tumour, hepatic parenchyma, and spleen were measured three times each and averaged. The ADC ratio of the tumour versus the surrounding liver parenchyma (ADC of the HCC/ADC of the liver parenchyma), and the normalised ADC value of the tumour (ADC value of the HCC/ADC value of the spleen) were then calculated. The average value of the mean tumour ADC, minimum tumour ADC, ADC ratio of the tumour versus the surrounding liver parenchyma (hereafter, ADC ratio of the tumour), and the normalised ADC value of the tumour were obtained and correlated with the histopathological parameters.

At the second session, two radiologists, one who participated in the first session and a second radiologist (D.I.C. with 8 years of experience in abdominal MRI interpretation), re-measured the ADC parameters of 30 consecutive HCCs in ascending order from the date of surgery using the aforementioned method used to evaluate the intra- and interobserver agreement of the ADC parameter measurements, 2 months after the first session.

Pathological evaluation

HCC specimens were retrieved and all tissue sections were sliced systematically into thin slices (5 mm). The slices were fixed in a 10% buffered formaldehyde solution and embedded in paraffin. In accordance with the guidelines developed by the Korean Liver Cancer Study Group for the Study of Primary Liver Cancer,[21] pathological reports for the HCCs were established by pathologists under the supervision of two experienced hepatic pathologists (C.K.P. and S.Y.H. with 32 and 5 years of experience in liver pathological interpretation, respectively). The original pathology reports were used for the acquisition of the following histopathological parameters: size, histological grade according to the grading system of Edmondson and Steiner,[22] percentage of fatty change, and presence of MVI of a tumour. When tumour differentiation was diverse within a single HCC, tumour differentiation of the majority portion was selected for histological grading of the lesion.

To evaluate the cellularity and degree of fibrosis and lymphocytic infiltration of the HCCs, digital images of histopathological haematoxylin and eosin-stained slides of tumours were obtained using ImageScope (Aperio, Vista, CA). A pathologist performed a preliminary review of all cases and established a pathological evaluation method to assess the cellularity and degree of fibrosis and lymphocytic infiltration of the HCCs. For tumours with diverse differentiation, cellularity was evaluated in the area of the dominant grade. Details regarding the pathological analysis of the cellularity and degree of fibrosis and lymphocytic infiltration of HCCs are provided in Electronic Supplementary Material Appendix E2.

Statistical analysis

All analyses were performed using SAS software (version 9.4). First, the intra- and interobserver agreement of the ADC parameter measurements were evaluated for 30 consecutive HCCs according to the date of surgery using intra- and inter-class correlation coefficients (ICCs). An ICC of >0.75 was indicative of good agreement.[23]

Pairwise comparisons to evaluate the differences in cellularity according to the histological grade were performed using the Mann–Whitney *U*-test; *p*-values that were less than the Bonferroni-corrected significance value of 0.017 (0.05/3) for all possible pairs were considered to indicate a significant difference.

Associations between the histopathological parameters (cellularity, histological grade, presence of MVI, degree of fibrosis, and lymphocyte infiltration) and ADC parameters (mean ADC, minimum ADC, ADC ratio, and normalised ADC of the tumour) of the tumours were assessed using linear regression analysis for continuous variables, and the Wilcoxon rank sum test or Spearman's rank correlation coefficient for ordinal variables. Of 143 tumours, 38 (26.6%) exhibited fatty change; 26 (68.4%) of these exhibited fatty change of $\leq$5% and the remaining 12 (31.6%) exhibited fatty change of 10–50%. In consideration of these distributions, the tumours were first divided into two groups: tumours with 10–50% fatty change and tumours with $\leq$5% fatty change. When a significant difference was found between these two groups for ADC parameters of the tumour using linear regression analysis, the association between fatty change and tumour ADC parameters was evaluated for tumours with fatty change of 10–50%. For multivariate analysis, parameters with a *p*-value of $\leq$0.20 in the univariate analysis were evaluated. Stepwise linear regression analysis was performed, until all remaining variables had *p*-values of $\leq$0.05.

To determine the interaction between the histopathological parameters and ADC parameters of the tumours, all main effects of the selected variables were considered with *p*-values of $<$0.2 from the univariate analysis and their interaction effects as a full model. Starting with the full model, the insignificant effects were eliminated and then the reduced model was fitted. This procedure was repeated until all effects in the current model were significant. A *p*-

Table 2
Clinical characteristics of the study patients.

Variable	Total (n=143)
Age, years mean (range)	57 (31–84)
Male: female ratio	105:38
Nodule size, mean (range) (cm)	1.7 (1.0–2.0)
Histological grade	
Edmondson grade I	9
Edmondson grade II	122
Edmondson grade III	12
Tumour marker (AFP)[a]	8.9 (1.3–4477.5)
Cause of cirrhosis	
Hepatitis B	125
Hepatitis C	11
Alcoholism	4
Others	3

AFP, alpha fetoprotein.
[a] Data are medians, with ranges.

Table 3
Intra-and interobserver agreement for ADC measurement.

Parameters	Intra-observer	Interobserver
	ICC (95% CI)	ICC (95% CI)
Mean ADC	0.987 (0.974, 0.994)	0.952 (0.903, 0.976)
Minimum ADC	0.984 (0.966, 0.992)	0.938 (0.877, 0.969)
ADC ratio	0.976 (0.950, 0.988)	0.908 (0.820, 0.954)
Normalised ADC	0.982 (0.964, 0.991)	0.930 (0.861, 0.965)

value of <0.05 was considered indicative of a statistically significant difference except when otherwise mentioned.

Results

An initial 165 patients met the inclusion criteria. Of them, 22 were excluded due to poor image quality (n=17) caused by patient movement, image noise, or left subphrenic location of tumours accompanied by cardiac motion artefact, or considerable tumour necrosis or haemorrhage (n=5) leading to difficulty in ADC value measurement. Finally, a total of 143 patients (105 men and 38 women; age range, 31–84 years; mean age, 57 years) with 143 HCCs (mean size, 1.7 cm; range, 1–2 cm) were included in this study. All included patients had liver cirrhosis of Child–Pugh class A and the most common cause of cirrhosis was chronic hepatitis B (125 patients). Among the 143 patients, 35 underwent lobectomy, 108 underwent segmentectomy, bisegmentectomy, or wedge resection. The mean and range of the time interval between surgery and MRI was 18 days and 1–60 days, respectively. The clinical and demographic data of the study groups are presented in Table 2.

The intra- and interobserver ICCs calculated for the ADC parameters ranged from 0.908 to 0.987 (Table 3). The mean cellularity of nine Edmondson grade I, 122 Edmondson grade II, and 12 Edmondson grade III HCCs were 775±218

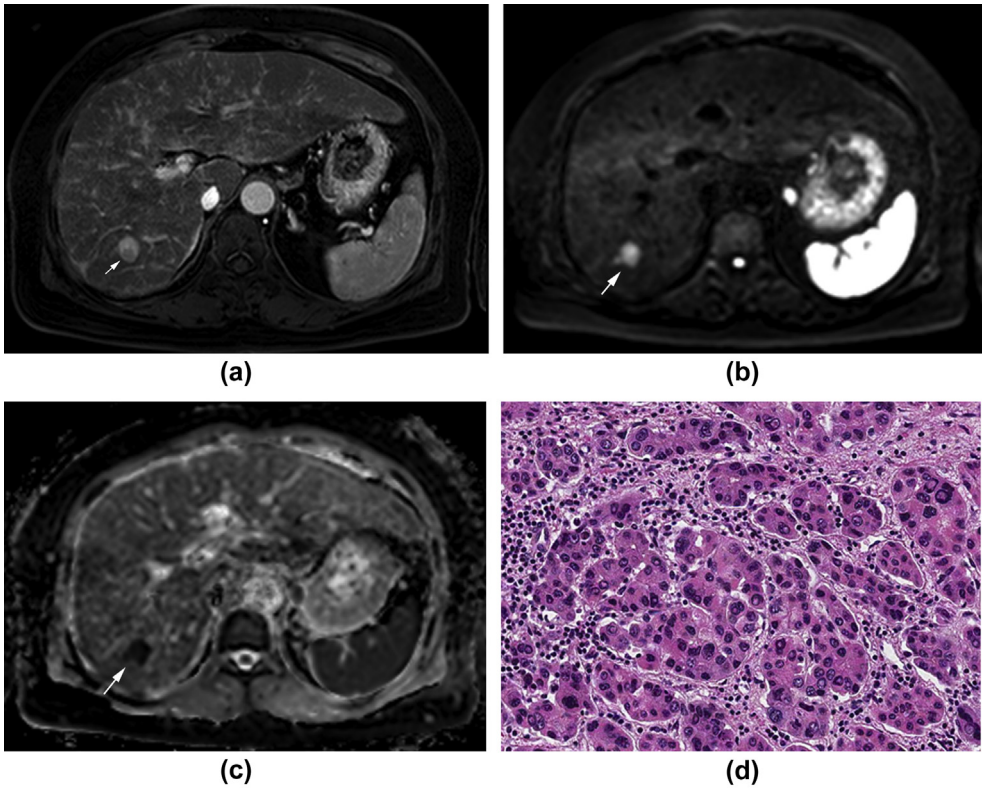

Figure 1 Images of a 54-year-old woman with HCC (Edmondson grade II). (a) Axial arterial phase image indicating a hypervascular tumour (arrow). The tumour (arrows) appeared as a hyperintensity on the DWI image (b) and marked hypointensity on the ADC map (c). The average mean and minimum ADC values, ADC ratio, and normalised ADC of the tumour were 0.32×10^{-3} mm^2/s, 0.20×10^{-3} mm^2/s, 0.31, and 0.48, respectively. (d) A photomicrograph (original magnification, ×100; haematoxylin and eosin stain) of the tumour revealed remarkable lymphocyte infiltration (grade 3). The summed cell count was 690. Histopathologically, microvascular invasion was not present.

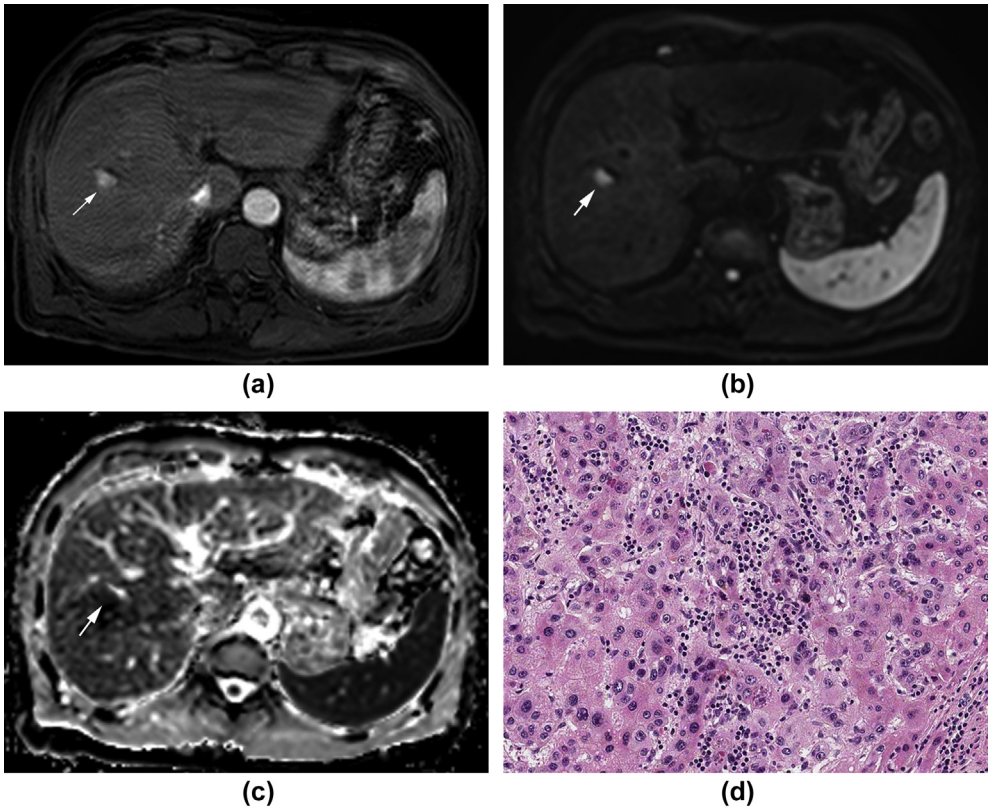

Figure 2 Images of a 56-year-old man with HCC (Edmondson grade I). (a)Axial arterial phase image indicating a hypervascular tumour (arrow). The tumour (arrows) appeared as a hyperintensity on the DWI image (b) and mild hypointensity on the ADC map (c). The average mean and minimum ADC values, ADC ratio, and normalised ADC of the tumour were 0.73×10^{-3} mm^2/s, 0.68×10^{-3} mm^2/s, 0.75, and 1.14, respectively. (d) A photomicrograph (original magnification, ×100; haematoxylin and eosin stain) of the tumour revealed remarkable lymphocyte infiltration (grade 3). The summed cell count was 525. Histopathologically, microvascular invasion was not present.

(range, 503–1,099), 765±277 (range, 345–1,858), and 727±242 (range, 444–1,200), respectively, and no significant difference was found between the cellularity and tumour grade (grade I versus II, p=0.72; I versus III, p=0.65; II versus III, p=0.68). No correlation was found between the cellularity and tumour ADC parameters (p=0.096–0.592; Figs 1 and 2).

The values of the tumour ADC parameters according to the tumour grade, absence or presence of MVI, and degree of fibrosis and lymphocyte infiltration are provided in Table 4. Although the minimum ADC, ADC ratio, and normalised ADC decreased as the tumour histological grade increased, there was only a tendency of low minimum ADC values for tumours with high grades (p=0.08; Figs 3 and 4). For MVI, the HCCs with MVI had significantly lower ADC ratios than did the HCCs without MVI (p=0.017), and the ADC ratio was also an independent parameter associated with MVI in the multivariate analysis (p=0.034). For fibrosis of the tumour, there was a significant negative correlation between the degree of fibrosis and the ADC ratio (p=0.042) only in the univariate analysis. For lymphocyte infiltration within a tumour, there was significant negative correlation between the degree of lymphocyte infiltration and the mean ADC and ADC ratio (p=0.049 and 0.002, respectively), and the mean ADC and ADC ratio were also independent parameters associated with lymphocyte infiltration in the multivariate analysis (p=0.009 and <0.001, respectively; Figs 1 and 2). In contrast, the fatty change in the tumour and ADC parameters were not significantly correlated (p>0.1).

Discussion

In the present study, there was no significant correlation between the tumour grade and ADC parameters (p>0.05), and the cellularity of the HCCs was not correlated with tumour grade or ADC parameters (p>0.05). With regard to MVI, only the ADC ratio was significantly associated with the presence of MVI of small HCCs (p<0.05). Meanwhile, there were significant relationships between lymphocyte infiltration and the mean ADC and ADC ratio of small HCCs (p<0.05). Considering the results of this study, it may be assumed that the conflicting results regarding the association between the ADC parameters and the histological grade or MVI of HCCs reported by previous studies[8–10] could be due to neglecting the effects of various extracellular components of HCCs, particularly the effect of lymphocyte infiltration on ADC parameters.

According to previous studies, patients undergoing hepatic resection for HCC with prominent lymphocyte

Table 4
ADC values and ratio according to histopathological parameters.

Parameters (Total n=143)	ADC value ($\times10^{-3}$mm^2/s)		ADC ratio	Normalised ADC
	Mean	Minimum		
Edmondson grade				
I (n=9)	1.14±0.37 (0.74–2.05)	1.01±0.35 (0.68–1.90)	0.9±0.15 (0.74–1.15)	1.47±0.54 (1.05–2.79)
II (n=122)	1.01±0.25 (0.32–1.95)	0.82±0.24 (0.13–1.74)	0.86±0.21 (0.26–1.48)	1.33±0.33 (0.39–2.72)
III (n=12)	1.02±0.28 (0.50–1.51)	0.76±0.22 (0.34–1.19)	0.81±0.18 (0.44–1.14)	1.25±0.33 (0.63–1.72)
p-Value, univariate analysis	0.35	0.08	0.31	0.51
p-Value, multivariate analysis	–	0.057	–	–
Microvascular invasion				
Absent (n=74)	1.05±0.24 (0.32–2.05)	0.85±0.24 (0.20–1.90)	0.89±0.19 (0.31–1.31)	1.36±0.32 (0.48–2.79)
Present (n=69)	1.00±0.28 (0.34–1.95)	0.80±0.26 (0.13–1.74)	0.83±0.21 (0.26–1.48)	1.3±0.37 (0.39–2.72)
p-Value, univariate analysis	0.071	0.28	0.017	0.18
p-Value, multivariate analysis	–	–	0.034	0.43
Fibrosis				
No (n=22)	1.07±0.34 (0.34–2.05)	0.84±0.35 (0.13–1.9)	0.91±0.25 (0.26–1.31)	1.38±0.45 (0.39–2.79)
Grade 1 (n=30)	1.04±0.2 (0.73–1.6)	0.86±0.19 (0.52–1.29)	0.9±0.15 (0.61–1.14)	1.36±0.29 (0.98–2.12)
Grade 2 (n=21)	0.96±0.23 (0.32–1.44)	0.77±0.24 (0.2–1.31)	0.81±0.19 (0.31–1.1)	1.3±0.33 (0.48–1.95)
Grade 3 (n=70)	1.02±0.26 (0.35–1.95)	0.83±0.24 (0.19–1.74)	0.84±0.2 (0.33–1.48)	1.32±0.34 (0.53–2.72)
p-Value, univariate analysis	0.37	0.84	0.042	0.59
p-Value, multivariate analysis	–	–	0.569	–
Lymphocyte infiltration				
No (n=26)	1.09±0.29 (0.66–1.95)	0.9±0.25 (0.42–1.47)	0.97±0.23 (0.61–1.48)	1.45±0.41 (0.94–2.72)
Grade 1 (n=39)	1.06±0.25 (0.34–1.92)	0.86±0.25 (0.13–1.74)	0.88±0.18 (0.26–1.12)	1.33±0.28 (0.39–1.89)
Grade 2 (n=22)	1.05±0.27 (0.69–2.05)	0.84±0.29 (0.43–1.9)	0.86±0.15 (0.6–1.14)	1.4±0.41 (1.01–2.79)
Grade 3 (n=56)	0.96±0.24 (0.32–1.6)	0.77±0.23 (0.19–1.29)	0.79±0.2 (0.31–1.22)	1.26±0.32 (0.48–1.84)
p-Value, univariate analysis	0.049	0.051	0.002	0.10
p-Value, multivariate analysis	0.009	0.057	<.0.001	0.09

Data are mean ± standard deviation (range).
Statistically significant as determined with Wilcoxon rank sum test for microvascular invasion, and Spearman's correlation analysis for the rest of the parameters (p<.05).

infiltration experienced better survival and disease-free survival than did those with HCC without lymphocyte infiltration.[24,25] Immunotherapy is a promising treatment option for HCC[26,27]; however, lymphocyte infiltration can result in reduced ADC parameters, as exhibited by aggressive tumours.[28,29] Therefore, using ADC parameters as an indicator of tumour aggressiveness in HCCs with high lymphocyte infiltration may be limited. To date, a detailed study of the incidence of HCCs with lymphocyte infiltration has not been performed. Wada *et al.* reported that 11 (7%) of 163 patients with HCCs of <3 cm in diameter exhibited marked lymphocyte infiltration of HCCs.[25] In the present study, 56 (39.2%) of 143 HCCs exhibited grade 3 intratumoural lymphocyte infiltration according to the present pathological criteria. Even considering the differences in pathological criteria, there is a wide gap in the incidence of high lymphocyte infiltration within HCCs between the study by Wada *et al.*[25] and the present study. This may be due to the difference in the size of the included lesions, as in the present HCCs with diameters between 10 and 20 mm were included. Therefore, using ADC parameters to predict tumour aggressiveness of small HCCs could be limited. Therefore, further sophisticated studies are required to elucidate the effects of lymphocyte infiltration of HCCs on ADC parameters.

In a recent meta-analysis regarding the correlation between the mean ADC and cellularity in different tumours based on a large sample,[30] the mean ADC correlated well with the cell count in glioma, ovarian cancer, and lung cancer, but not in lymphoma. The authors suggested that cell count together with other histopathological features, such as the extracellular matrix, nucleic areas, stroma/parenchyma ratio, and/or microvessel density, could be attributed to the results. In the present study, the cellularity of the HCCs did not correlate with the ADC parameters, nor did it correlate with the tumour grade (p>0.05). In a previous study by Suh *et al.*,[13] the mean ADC values were significantly lower for grade II HCCs with MVI than for grade II HCCs without MVI. Therefore, if a study population contains many tumours with the same histological grade, the ADC parameters may be affected by factors such as MVI rather than the tumour grade itself.[13] Recently, a β-catenin mutation and cytokeratin 19-positive HCCs were also found to be significantly associated with the mean ADC of the tumour and the tumour-to-liver ADC ratio, respectively.[31,32]

Normalisation of the ADC using a reference organ or adjacent normal parenchyma (i.e., the ADC ratio of the tumour versus that of the liver) has been used to improve reproducibility[33]; however, a constant tendency of absolute ADC values and normalised ADC values against histopathological parameters of HCCs was not identified in the present study. In addition, the ADC is influenced by diverse MRI systems (e.g., the hardware/software platform, DWI sequence, and acquisition parameters, and individual scanner idiosyncrasies), human, or biological factors (patient size, shape, and cooperativeness; or lesion

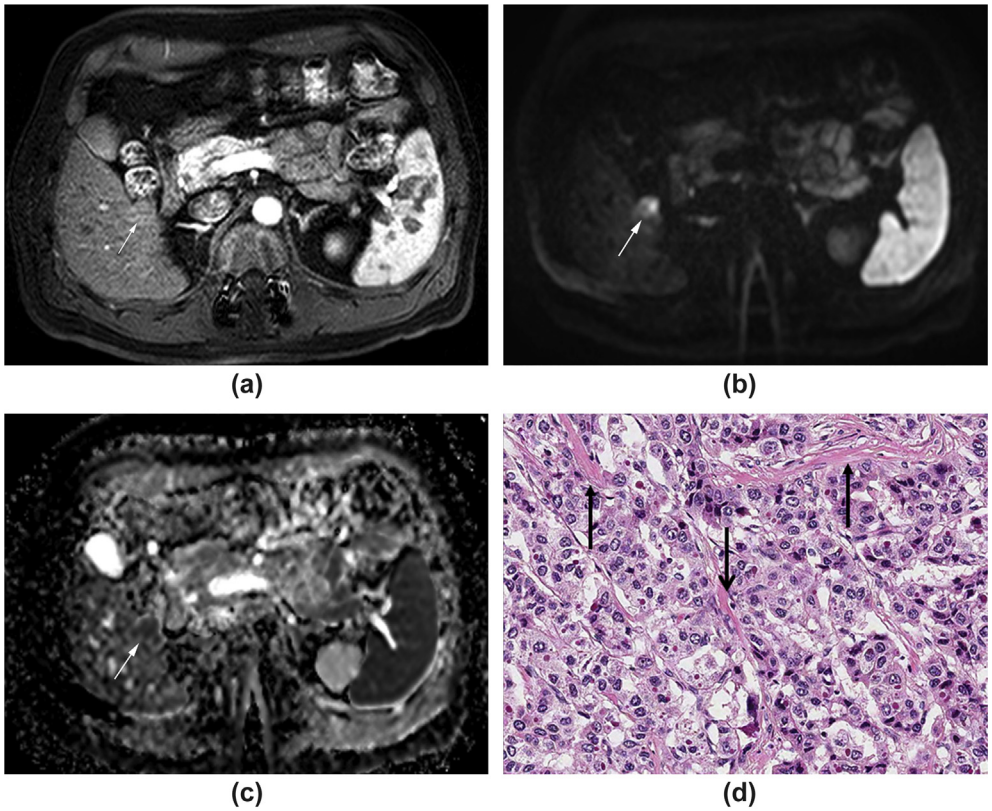

Figure 3 Images of a 52-year-old man with HCC (Edmondson grade III). (a) Axial arterial phase image indicating a mild hypervascular tumour (arrow). The tumour (arrows) appeared as a hyperintensity on the DWI image (b) and mild hypointensity on the ADC map (c). The average mean and minimum ADC values, ADC ratio, and normalised ADC of the tumour were 0.87×10^{-3} mm^2/s, 0.66×10^{-3} mm^2/s, 0.81, and 1.24, respectively. (d) A photomicrograph (original magnification, ×100; haematoxylin and eosin stain) of the tumour revealed fibrotic stroma (arrows) without lymphocyte infiltration (grade 0). The summed cell count was 1175. Histopathologically, microvascular invasion was present.

location and heterogeneity), algorithms used to convert DWI to ADC, the radiologist's definition of measurement region, and also inherently low signal-to-noise ratios. It is also susceptible to a range of DWI artefacts.[2,34] Accordingly, there are many potential limitations associated with predicting tumour aggressiveness using ADC parameters. To resolve this, multiple institutions would need to participate in standardising the DWI sequence and the acquisition parameters as fully as possible. Then, a large sophisticated prospective study would be necessary to clarify the significance of ADC parameters for the prediction of HCC aggressiveness.

Recently, intravoxel incoherent motion DWI has been studied for the prediction of high-grade HCC[35,36]; however, these studies did not consider the possibility of confounding effects from tumour components other than tumour cells. To investigate the precise role of DWI-derived parameters for the prediction of aggressive HCCs, it might be necessary to assess these confounding effects, particularly that of intratumoural lymphocyte infiltration, relevant to the prognosis of HCC.

This study has some limitations. First, selection and verification biases may have occurred due to the retrospective nature of the study. Second, due to the small number of Edmondson grade I and III HCCs, evaluating the overall interaction between tumour grades and ADC parameters may have been limited. Third, in this study, tumours were differentiated based on the histological grade of the majority portion in tumours with diverse differentiation. Although the minimum ADC of the tumour could be correlated with the highest grade within the tumour, whether a hand-drawn ROI will accurately include areas with the highest grade of the tumour remains uncertain. Therefore, tumour differentiation using the majority portion was selected to correlate with the minimum ADC of the tumour. Fourth, the effect of liver cirrhosis on the ADC value of the spleen was not considered. The splenic ADC value of cirrhotic patients with advanced portal hypertension and splenomegaly may differ from that of cirrhotic patients with mild or no portal hypertension[20]; however, it is assumed that because all 143 patients had Child–Pugh class A, the ADC variability of the spleen associated with portal hypertension and splenomegaly in patients was small.

In conclusion, the tumour grade of small HCCs was not correlated with ADC parameters. The tumour-to-liver ADC ratio was a significant independent parameter for lymphocyte infiltration and MVI of small HCCs.

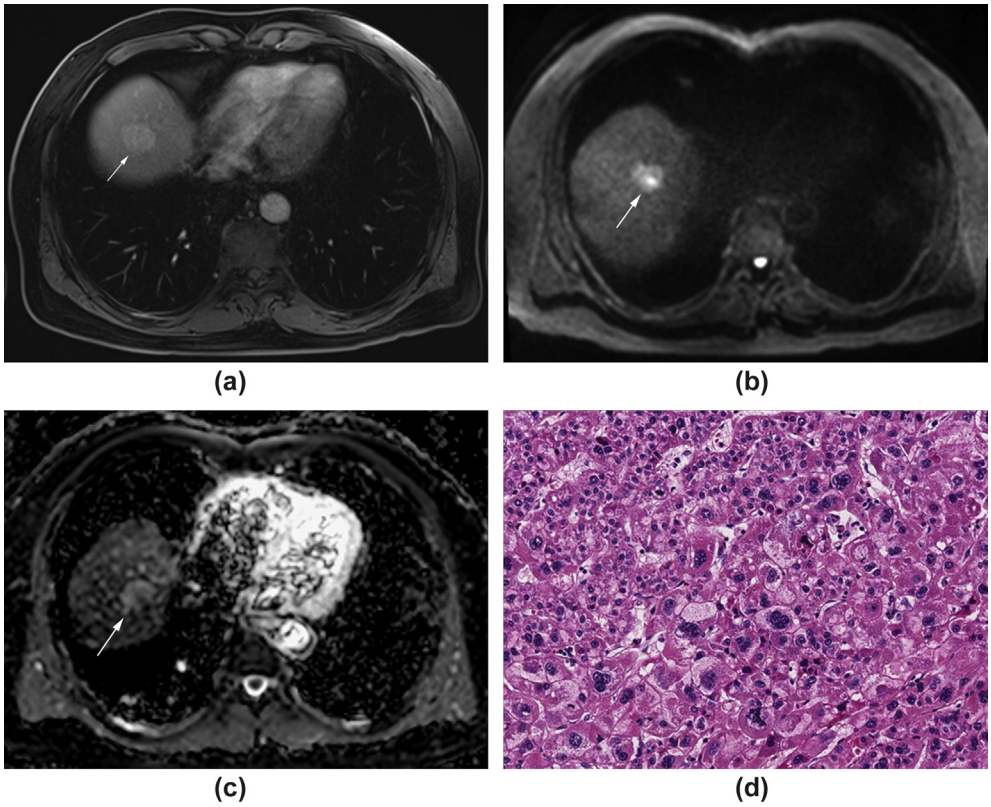

Figure 4 Images of a 58-year-old man with HCC (Edmondson grade III). (a) Axial arterial phase image indicating a hypervascular tumour in the liver dome (arrow). The tumour (arrows) appeared as a hyperintensity on the DWI image (b) and mild hyperintensity on the ADC map (c). The average mean and minimum ADC values, ADC ratio, and normalised ADC of the tumour were 1.59×10^{-3} mm^2/s, 0.97×10^{-3} mm^2/s, 1.03, and 1.72, respectively. (d) A photomicrograph (original magnification, ×100; haematoxylin and eosin stain) of the tumour revealed few lymphocytes (grade 1) (arrows). The summed cell count was 785. Histopathologically, microvascular invasion was present.

Conflict of interest

The authors declare no conflict of interest.

Acknowledgements

The authors thank Park CK and Ha SY for original pathologic reports of the included patients in this paper.

Appendix A. Supplementary data

Supplementary data to this article can be found online at https://doi.org/10.1016/j.crad.2019.01.019.

References

1. Karaosmanoglu AD, Onur MR, Ozmen MN, *et al*. Magnetic resonance imaging of liver metastasis. *Semin Ultrasound CT MR* 2016;**37**:533–48.
2. Taouli B, Koh DM. Diffusion-weighted MR imaging of the liver. *Radiology* 2010;**254**:47–66.
3. Park MJ, Kim YK, Lee MW, *et al*. Small hepatocellular carcinomas: improved sensitivity by combining gadoxetic acid-enhanced and diffusion-weighted MR imaging patterns. *Radiology* 2012;**264**:761–70.
4. Taouli B, Vilgrain V, Dumont E, *et al*. Evaluation of liver diffusion isotropy and characterization of focal hepatic lesions with two single-shot echo-planar MR imaging sequences: prospective study in 66 patients. *Radiology* 2003;**226**:71–8.
5. Parikh T, Drew SJ, Lee VS, *et al*. Focal liver lesion detection and characterization with diffusion-weighted MR imaging: comparison with standard breath-hold T2-weighted imaging. *Radiology* 2008;**246**:812–22.
6. Hwang J, Kim YK, Kim JM, *et al*. Pretransplant diagnosis of hepatocellular carcinoma by gadoxetic acid-enhanced and diffusion-weighted magnetic resonance imaging. *Liver Transpl* 2014;**20**:1436–46.
7. Malayeri AA, El Khouli RH, Zaheer A, *et al*. Principles and applications of diffusion-weighted imaging in cancer detection, staging, and treatment follow-up. *RadioGraphics* 2011;**31**:1773–91.
8. An C, Park MS, Jeon HM, *et al*. Prediction of the histopathological grade of hepatocellular carcinoma using qualitative diffusion-weighted, dynamic, and hepatobiliary phase MRI. *Eur Radiol* 2012;**22**:1701–8.
9. Heo SH, Jeong YY, Shin SS, *et al*. Apparent diffusion coefficient value of diffusion-weighted imaging for hepatocellular carcinoma: correlation with the histologic differentiation and the expression of vascular endothelial growth factor. *Kor J Radiol* 2010;**11**:295–303.
10. Muhi A, Ichikawa T, Motosugi U, *et al*. High-b-value diffusion-weighted MR imaging of hepatocellular lesions: estimation of grade of malignancy of hepatocellular carcinoma. *J Magn Reson Imag* 2009;**30**:1005–11.
11. Nakanishi M, Chuma M, Hige S, *et al*. Relationship between diffusion-weighted magnetic resonance imaging and histological tumor grading of hepatocellular carcinoma. *Ann Surg Oncol* 2012;**19**:1302–9.
12. Nishie A, Tajima T, Asayama Y, *et al*. Diagnostic performance of apparent diffusion coefficient for predicting histological grade of hepatocellular carcinoma. *Eur J Radiol* 2011;**80**:e29–33.
13. Suh YJ, Kim MJ, Choi JY, *et al*. Preoperative prediction of the microvascular invasion of hepatocellular carcinoma with diffusion-weighted imaging. *Liver Transpl* 2012;**18**:1171–8.
14. Nasu K, Kuroki Y, Tsukamoto T, *et al*. Diffusion-weighted imaging of surgically resected hepatocellular carcinoma: imaging characteristics

and relationship among signal intensity, apparent diffusion coefficient, and histopathologic grade. *AJR Am J Roentgenol* 2009;**193**:438–44.
15. Boussouar S, Itti E, Lin SJ, *et al*. Functional imaging of hepatocellular carcinoma using diffusion-weighted MRI and (18)F-FDG PET/CT in patients on waiting-list for liver transplantation. *Cancer Imag* 2016;**16**:4.
16. An C, Kim DW, Park YN, *et al*. Single hepatocellular carcinoma: preoperative MR imaging to predict early recurrence after curative resection. *Radiology* 2015;**276**:433–43.
17. Schlageter M, Terracciano LM, D'Angelo S, *et al*. Histopathology of hepatocellular carcinoma. *World J Gastroenterol* 2014;**20**:15955–64.
18. Taouli B, Chouli M, Martin AJ, *et al*. Chronic hepatitis: role of diffusion-weighted imaging and diffusion tensor imaging for the diagnosis of liver fibrosis and inflammation. *J Magn Reson Imag* 2008;**28**:89–95.
19. Namimoto T, Nakagawa M, Kizaki Y, *et al*. Characterization of liver tumors by diffusion-weighted imaging: comparison of diagnostic performance using the mean and minimum apparent diffusion coefficient. *J Comput Assist Tomogr* 2015;**39**:453–61.
20. Song JS, Kwak HS, Byon JH, *et al*. Diffusion-weighted MR imaging of upper abdominal organs at different time points: apparent diffusion coefficient normalization using a reference organ. *J Magn Reson Imag* 2017 May;**45**(5):1494–501.
21. 2014 Korean liver cancer study group-national cancer center Korea practice guideline for the management of hepatocellular carcinoma. *Kor J Radiol* 2015;**16**:465–522.
22. Edmondson HA, Steiner PE. Primary carcinoma of the liver: a study of 100 cases among 48,900 necropsies. *Cancer* 1954;**7**:462–503.
23. Chen X, Qin L, Pan D, *et al*. Liver diffusion-weighted MR imaging: reproducibility comparison of ADC measurements obtained with multiple breath-hold, free-breathing, respiratory-triggered, and navigator-triggered techniques. *Radiology* 2014;**271**:113–25.
24. Shirabe K, Matsumata T, Maeda T, *et al*. A long-term surviving patient with hepatocellular carcinoma including lymphocytes infiltration—a clinicopathological study. *Hepatogastroenterology* 1995;**42**:996–1001.
25. Wada Y, Nakashima O, Kutami R, *et al*. Clinicopathological study on hepatocellular carcinoma with lymphocytic infiltration. *Hepatology* 1998;**27**:407–14.
26. Gbolahan OB, Schacht MA, Beckley EW, *et al*. Locoregional and systemic therapy for hepatocellular carcinoma. *J Gastrointest Oncol* 2017;**8**:215–28.
27. Desai JR, Ochoa S, Prins PA, *et al*. Systemic therapy for advanced hepatocellular carcinoma: an update. *J Gastrointest Oncol* 2017;**8**:243–55.
28. Cao W, Liang C, Gen Y, *et al*. Role of diffusion-weighted imaging for detecting bone marrow infiltration in skull in children with acute lymphoblastic leukemia. *Diagn Interv Radiol* 2016;**22**:580–6.
29. Shin HJ, Kim SH, Lee HJ, *et al*. Tumor apparent diffusion coefficient as an imaging biomarker to predict tumor aggressiveness in patients with estrogen-receptor-positive breast cancer. *NMR Biomed* 2016;**29**:1070–8.
30. Surov A, Meyer HJ, Wienke A. Correlation between apparent diffusion coefficient (ADC) and cellularity is different in several tumors: a meta-analysis. *Oncotarget* 2017;**8**:59492–9.
31. Kitao A, Matsui O, Yoneda N, *et al*. Hepatocellular carcinoma with beta-catenin mutation: imaging and pathologic characteristics. *Radiology* 2015;**275**:708–17.
32. Choi SY, Kim SH, Park CK, *et al*. Imaging features of gadoxetic acid-enhanced and diffusion-weighted MR imaging for identifying cytokeratin 19-positive hepatocellular carcinoma: a retrospective observational study. *Radiology* 2017:162846.
33. Zhu J, Zhang J, Gao JY, *et al*. Apparent diffusion coefficient normalization of normal liver: will it improve the reproducibility of diffusion-weighted imaging at different MR scanners as a new biomarker? *Medicine (Baltimore)* 2017;**96**:e5910.
34. Taouli B, Beer AJ, Chenevert T, *et al*. Diffusion-weighted imaging outside the brain: consensus statement from an ISMRM-sponsored workshop. *J Magn Reson Imag* 2016;**44**:521–40.
35. Granata V, Fusco R, Catalano O, *et al*. Intravoxel incoherent motion (IVIM) in diffusion-weighted imaging (DWI) for hepatocellular carcinoma: correlation with histologic grade. *Oncotarget* 2016;**7**:79357–64.
36. Woo S, Lee JM, Yoon JH, *et al*. Intravoxel incoherent motion diffusion-weighted MR imaging of hepatocellular carcinoma: correlation with enhancement degree and histologic grade. *Radiology* 2014;**270**:758–67.